High-precision, all-electron, full-potential calculation of the equation of state and elastic constants of corundum

J. C. Boettger
Theoretical Division, Los Alamos National Laboratory, Los Alamos, New Mexico 87545
(Received 12 August 1996)

The all-electron, full-potential linear combinations of Gaussian type orbitals–fitting function technique has been used to perform high-precision total-energy calculations on α-alumina (corundum). The calculations yield zero-pressure lattice parameters that are in 0.3% agreement with experiment and symmetry-preserving elastic constants that agree with experiment to within 5%. The bulk modulus and pressure derivatives of the lattice parameters are also in good agreement with existing data. The calculated energies have been used to generate an analytical equation of state (EOS) for corundum that should be valid up to at least 250 GPa. The fitted EOS agrees with room temperature diamond anvil cell data up to 175 GPa to within the known limitations of the experimental data. The c/a ratio, band gap, and tetragonal shear modulus have been determined for pressures up to 250 GPa. The c/a ratio varies by less than 3% over the entire pressure range. For pressures above 150 GPa, the band gap changes from direct to indirect and the tetragonal shear modulus softens. The linear pressure coefficient of the band gap is estimated to be 5.1 meV/kbar at zero pressure. [S0163-1829(97)03602-3]

I. INTRODUCTION

Corundum (α-Al_2O_3; α-alumina) is of great technological importance both in its pure form (sapphire) and Cr-doped form (ruby) with applications in industrial areas including optics, electronics, and ceramics. Corundum is significant to geophysicists as an abundant crustal material. High-pressure physicists often use sapphire as a window material during shock-wave experiments, while ruby is a standard pressure calibrant for diamond anvil cell (DAC) experiments. Because of these many applications, especially those related to geophysics and high-pressure research, considerable effort has been devoted to measuring the equation of state[1–6] (EOS) and elastic constants[7–9] of corundum. There also have been a number of lattice dynamical calculations devoted to the EOS and/or elasticity of corundum using various model potentials.[10–17]

Corundum poses a significant challenge to electronic structure theorists because of the complexity of the α-Al_2O_3 structure,[18] which includes two formula units per primitive cell. For this reason, early electronic structure calculations focussed on the electronic energy bands and optical properties without any attempt to calculate the total energy.[19] As time has passed, however, computer technology and software have developed rapidly allowing successively more precise electronic structure calculations. In 1991, Salasco *et al.*[20] determined all four lattice parameters for corundum by minimizing the Hartree-Fock total energy using the linear combinations of Gaussian type orbitals (LCGTO) technique with a rather small GTO basis set. In 1994, Ching and Xu[21] used the orthogonalized (frozen-core) linear combinations of atomic orbitals (OLCAO) method to calculate the lattice parameters and bulk modulus of corundum within the local density approximation (LDA) to density functional theory. That same year, Marton and Cohen[22] used the all-electron, full-potential (LDA) linearized augmented-plane-wave +local orbitals (LAPW+LO) technique to calculate EOS's for alumina in the α-Al_2O_3 and Rh_2O_3(II) structures, assuming both lattices vary isotropically with pressure. It appears that electronic structure calculations have not been applied to the elastic constants of corundum.

In the present investigation, the all-electron, full-potential linear combinations of Gaussian type orbitals–fitting function (LCGTO-FF) technique has been used to perform high-precision LDA total energy calculations on corundum for various combinations of the hexagonal lattice parameters a and c. Those energies were then fitted with analytical functions to extract the lattice parameters, cohesive energy, symmetry-preserving elastic constants, and EOS. In the next section, the structure of corundum will be described. In Sec. III, the basis sets used and other technical details of the calculations will be discussed briefly. Results will be presented, and compared with experimental data and previous calculations in Sec. IV. A few concluding remarks will be given in the final section.

II. CRYSTAL STRUCTURE

The α-alumina structure is rhombohedral with two formula units of Al_2O_3 in each primitive cell, and has $D^6_{3d}(R3c)$ symmetry. The three primitive lattice vectors have equal lengths (a_R) and are separated by equal angles (α_R). The lattice may also be viewed as a hexagonal lattice containing six formula units per cell with lattice parameters a and c, where the c-axis is the threefold axis of the primitive rhombohedral cell and c is the length of the primitive cell along that axis.

The origin of the lattice may be chosen to be an inversion center. In that case, the four Al atoms in the unit cell lie on the c-axis with one pair of atoms above the origin and the other below, and with the center of each pair at a distance of $0.25c$ from the origin. Each pair of Al atoms can be associated with three O atoms located at the vertices of an equilateral triangle centered on the midpoint of the line connecting the two Al atoms. The three O atoms that lie below the origin

are rotated by 60° relative to those above the origin, thereby preserving the inversion symmetry of the lattice. Neighboring cells supply each Al atom with three additional O neighbors, slightly farther away than the three nearest neighbors; i.e., the coordination of each Al atom is approximately sixfold. The positions of all ten atoms in the unit cell can be specified with two internal parameters; the distance in units of c from the origin to one of the Al atoms (u) and the distance in units of a from the c axis to each O atom (ν). A more detailed description of the structure for α-alumina, with diagrams, can be found in Wycoff.[18]

Under ambient conditions, the lattice parameters for corundum are given by Wyckoff[18] as $a_R=9.691$ bohrs, $\alpha_R=55°\,20'$, $a=9.0008$ bohrs, $c=24.572$ bohrs, $u=0.352$, and $\nu=0.306$. Although there have been more recent measurements of these parameters,[1,2] the newer values do not differ significantly. Hence the Wyckoff values have been used as the starting point for the present calculations.

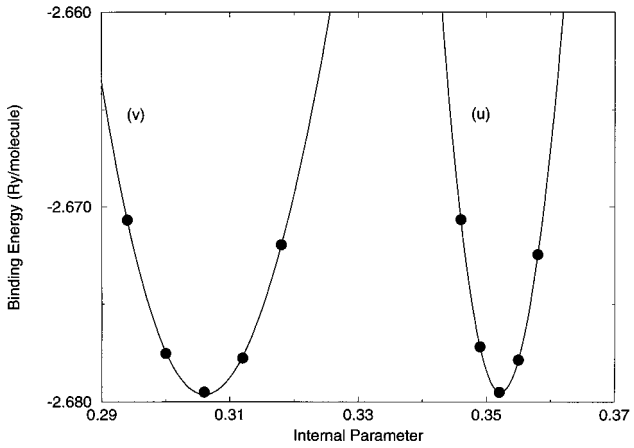

FIG. 1. Calculated binding energies (Ry/molecule) and fitted binding curves as functions of the internal parameters u and v of corundum.

III. TECHNICAL DETAILS

The calculations reported here employed the all-electron, full-potential LCGTO-FF electronic structure technique as embodied in the program package GTOFF,[23] a generalization of the 2D electronic structure program FILMS (Refs. 24 and 25) to include 1D and 3D periodicities. The LCGTO-FF technique is distinguished from other electronic structure methods by its use of three independent GTO basis sets to expand the orbitals, charge density, and LDA exchange-correlation (XC) integral kernels; here using the LDA parametrization of Hedin and Lundqvist.[26] The charge fitting functions are used to reduce the total number of Coulomb integrals by replacing the usual four-center integrals in the total energy and one-electron equations with three-center integrals; thereby allowing high-precision calculations on relatively complex systems. The XC fit provides a simple yet sophisticated numerical quadrature scheme capable of producing accurate results with a rather coarse numerical integration mesh. The overall precision of any LCGTO-FF calculation will, of course, be largely determined by the selection of these three basis sets.

The orbital basis set used for the Al atoms was derived from the $11s7p$ atomic basis set of Huzinaga.[27] The basis set was first contracted into a $6s3p$ segmented basis set[28] using contraction coefficients determined from LDA atom calculations. That basis set was then augmented with a single d-type GTO with an exponent of 0.3, yielding a $6s3p1d$ orbital basis set similar to those used in recent LCGTO-FF calculations on Al crystals[29] and films.[30] The orbital basis set for the O atoms was derived in a similar fashion from Huzinaga's[27] $9s5p$ atomic basis set by contracting the primitive basis into a $4s2p$ segmented basis, replacing the smallest s-type exponent with two exponents (0.339 0762 and 0.15), and augmenting the basis set with one additional p-type GTO (exponent 0.15) and one d-type GTO (exponent 0.3); yielding a $5s3p1d$ basis. The exponents of the more diffuse GTO's in the orbital basis sets were adjusted slightly during some of the calculations to avoid near linear dependencies due to intersite overlap. Both of these basis sets are substantially richer than the $3s2p$ orbital basis sets used in the earlier LCGTO Hartree-Fock calculations.[20]

The D_{3d}^6 symmetry of the α-alumina structure ensures that the only types of fitting function GTO's allowed on the Al atoms (through $l=2$) are s, p_z, and $d_{z^2-1/2(x^2+y^2)}$. For the O atoms the allowed types can be reduced further by elimination of p_z-type GTO's. The charge fitting function basis sets for all ten atoms included nine s-type GTO's (exponents: 900.0, 240.0, 80.0, 27.0, 9.0, 3.0, 0.9, 0.35, 0.15) and two d-type GTO's (exponents: 0.9, 0.4). In addition, each of the six Al atoms was given two p-type charge functions (exponents: 1.0, 0.4). The XC fitting function basis sets for all ten atoms included six s-type GTO's (exponents: 80.0, 16.0, 3.8, 1.0, 0.35, 0.15) and two d-type GTO's (exponents: 0.9, 0.4). Once again, each Al basis was augmented with two p-type XC functions (exponents: 1.0, 0.4). The complete charge and XC basis sets thus include a total of 118 and 88 primitive GTO's per unit cell, respectively. The primitive charge (XC) basis functions were then contracted into 24 (18) symmetry adapted functions per cell; versus 194 orbital basis functions per cell. This ability to use symmetry to significantly reduce the size of a calculation is one of the advantages of the LCGTO-FF method over more traditional LCGTO methods.

All necessary Brillouin zone (BZ) integrations were carried out via the histogram method on a uniform $4\times4\times4$ mesh with 13 irreducible k points. For each calculation, the self-consistent field (SCF) cycle was iterated until the total energy changed by less than 1 μRy per atom.

IV. RESULTS

Given the computational resources required by each total energy calculation for corundum, simultaneous optimization of all four lattice parameters is not a practical option at this time. Previous calculations have addressed this problem either by optimizing each of the four parameters V, c/a, u, and ν independently, with the other three held fixed,[20,21] thereby obtaining the zero-pressure geometry, or by simply varying V isotropically to determine the high-pressure EOS and phase stability.[22] A somewhat more ambitious strategy has been employed for the current study.

In the first stage of this investigation, the parameters u and ν were optimized independently for $a_R=9.7$ bohrs and

TABLE I. Parameters for the generalized two dimensional cubic function [Eq. (1)] used to fit $E(a,c)$.

D_{30}	−0.302 042 95	D_{03}	−0.000 559 26
D_{21}	0.008 650 35	D_{12}	−0.034 485 59
D_{20}	0.941 267 60	D_{02}	0.046 604 93
D_{11}	0.122 372 77	D_{00}	−16.077 200 39
a_0	9.007 386 00	c_0	24.508 023 20

$c/a=2.73$. Total energies were calculated for five values of u, with ν fixed at 0.306, and for five values of ν, with u fixed at 0.352. Binding energies were then obtained by removing atomic energies for O (−149.049 471 Ry) and Al (−482.596 646 Ry), as calculated with GTOFF. Finally, those binding energies were fitted with cubic functions to determine the optimum values of u and ν; 0.352 and 0.306, respectively. These predicted internal lattice parameters are identical to the accepted experimental values.[1,2,18] The calculated binding energies (E_b) and fitted binding curves for both parameters are shown in Fig. 1. Since experimental data[1,2] indicate that u and ν are both insensitive to pressure, these internal parameters were fixed at their experimental values throughout the remainder of this investigation.

The two remaining independent lattice parameters, here chosen for convenience to be V and c/a, were varied simultaneously. Ten cell volumes ranging between 0.65 and 1.06 times the ambient volume were selected for consideration (1832.7677, 1777.7884, 1723.9197, 1671.1504, 1619.4691, 1568.8644, 1470.8396, 1376.9855, 1243.8259, and 1119.5402; all in bohr^3). For each volume, electronic structure calculations were carried out at four values of c/a (2.65, 2.69, 2.73, and 2.77 for the seven larger volumes and 2.61, 2.65, 2.69, and 2.73 for the three smaller volumes). Forty binding energies (E_b) and electronic energy band gaps (E_g) were generated in this manner.[31] In the remainder of this section, those results will be used to determine a number of properties for corundum.

A. Zero-pressure properties

To extract information about the low pressure properties of corundum, the 20 energies associated with the five larger volumes were least squares fitted to a generalized two-dimensional cubic function of a and c with the form

$$E(a,c)=\sum_{i=0}^{3}\sum_{j=0}^{3-i} D_{ij}(a-a_0)^i(c-c_0)^j, \qquad (1)$$

where a_0 and c_0 are the values of a and c at the local energy minimum that lies within the range of the data. From the variational principal, D_{10} and D_{01} must both be identically zero. The ten nonzero parameters obtained from the fit are listed in Table I. The quality of the fit to the data is exceptional, with a standard deviation of only 67 μRy/hex-cell (11 μRy/molecule) out of a fitted binding energy range of 6546 μRy/hex-cell, clearly indicating the numerical stability achieved with GTOFF.

The internal lattice parameters u and ν discussed above and the external lattice parameters a, c, c/a, and V_0 from the cubic fit [Eq. (1)] are compared with various theoretical and experimental results in Table II. The theoretical values include results from the three electronic structure investigations discussed earlier[20–22] and two lattice dynamical calculations[15] using the potential induced breathing (PIB) method; one using the Thomas-Fermi (TF) approximation to the electronic kinetic energy, and the other using the Kohn-Sham (KS) approximation. The experimental data include three sets of room temperature measurements[1,2,18] and two sets of 100 K estimates derived from the room temperature results using axially resolved thermal expansion data.[32] Axially averaged thermal expansion data ranging down to 20 K suggest that the lattice parameters of corundum should not vary significantly between 20 and 100 K.[33] The current lattice parameter predictions are in somewhat better agreement with the measured values than the earlier theoretical values.[15,20–22] In particular, the internal lattice parameters obtained here are in essentially perfect agreement with the

TABLE II. Comparison of theory and experiment for the internal lattice parameters (u and ν), hexagonal cell lattice constants (a and c; bohr), c/a ratio, and zero-pressure volume (V_0; bohr^3/molecule) for corundum.

Source	u	ν	a	c	c/a	V_0
PIB (TF) (Ref. 15)	0.361	0.296	9.147	23.69	2.59	286.1
PIB (KS) (Ref. 15)	0.357	0.301	8.984	24.08	2.68	280.5
LCGTO (Ref. 20)	0.354	0.304	8.955	24.61	2.748	284.88
OLCAO (Ref. 21)	0.355	0.312	9.136	23.84	2.61	287.3
LAPW+LO (Ref. 22)						282.0
LCGTO-FF (Present)	0.352	0.306	9.0074	24.508	2.721	287.00
Expt. 293 K (Ref. 1)	0.352	0.306	9.0059	24.585	2.730	287.81
Expt. 293 K (Ref. 2)	0.352	0.306	8.9964	24.556	2.730	286.86
Expt. 293 K (Ref. 18)	0.352	0.306	9.0008	24.572	2.730	287.33
Expt. 100 K[a]			9.0005	24.566	2.729	287.24
Expt. 100 K[b]			8.9910	24.537	2.729	286.30

[a]Values at 100 K obtained from the room temperature data of Ref. 1 by applying thermal expansion data from Ref. 32.

[b]Values at 100 K obtained from the room temperature data of Ref. 2 by applying thermal expansion data from Ref. 32.

TABLE III. Theoretical and experimental values for four symmetry-preserving elastic constants of corundum; $(C_{11}+C_{12})$, C_{33}, C_{13}, and C^t (in GPa). (LD=lattice dynamics.)

Source	$(C_{11}+C_{12})$	C_{33}	C_{13}	C^t
LD (Ref. 10)	464	449	73	178
LD (Ref. 11)	584.4	502.3	127.2	180.0
LD (Ref. 13)	759.5	507.2	119.1	216.2
LD (Ref. 13)	716.0	467.2	119.6	195.3
LD (Ref. 14)	697	455	130	181
LCGTO-FF (Present)	652.4	478.3	115.4	191.2
Expt. (Ref. 8)	660.2	501.8	117.2	199.2
Expt. (Ref. 9)	660.1	500.9	116.0	199.6

data, while the calculated zero-pressure volume lies between the two 100 K estimates. The largest discrepancy between the current results and the data is a small (0.3%) reduction in the c/a ratio, which is still the most accurate theoretical result to date. This level of agreement between theory and experiment is quite remarkable given the known tendency for LDA calculations to underestimate zero-pressure volumes. One other, possibly related, exception to this general rule is crystalline Al, for which nonrelativistic LDA theory and experiment are also in almost perfect agreement.[29]

The analytical form of Eq. (1) can be used to determine a number of additional properties of corundum via elastic theory. Three combinations of the six independent elastic constants can be determined from the second derivatives of $E(a,c)$, each associated with a symmetry-preserving distortion of the lattice;

$$C_{11}+C_{12}=\frac{a_0^2}{2V_0}\frac{\delta^2 E}{\delta a^2}, \tag{2}$$

$$C_{33}=\frac{c_0^2}{V_0}\frac{\delta^2 E}{\delta c^2}, \tag{3}$$

$$C_{13}=\frac{c_0 a_0}{2V_0}\frac{\delta^2 E}{\delta a\,\delta c}. \tag{4}$$

Resolution of C_{11} and C_{12} would require some symmetry breaking distortion, such as a uniaxial compression perpendicular to the c axis. One additional symmetry-preserving elastic constant that can be derived from those already given is the tetragonal shear modulus,

$$C^t=\frac{1}{6}\left[(C_{11}+C_{12})+2C_{33}-4C_{13}\right], \tag{5}$$

associated with volume conserving tetragonal distortions along the c axis.

The four symmetry-preserving elastic constants $(C_{11}+C_{12})$, C_{33}, C_{13}, and C^t obtained here are listed in Table III, along with results from lattice dynamical calculations using various model potentials[10,11,13,14] and two sets of experimental values[8,9] obtained under ambient conditions from vibrational response measurements. Once again, the current predictions are in better agreement with the data than are any of the earlier results. All of the calculated elastic constants agree with the measured values to within 5%, with the largest error being in C_{33}. This level of agreement is quite good for parameters that are determined from second derivatives of a fitted curve.

TABLE IV. Theoretical and experimental values for the bulk modulus (B; GPa) and pressure derivatives of the lattice parameters (a' and c'; GPa^{-1}) for corundum. (Present values are from a cubic fit.)

Source	B	a'	c'
PIB (TF) (Ref. 15)	264	−0.000 89	−0.001 09
PIB (KS) (Ref. 15)	356	−0.001 10	−0.001 46
OLCAO (Ref. 21)	242		
LAPW+LO (Ref. 22)	257		
LCGTO-FF (Present)	248.7	−0.001 27	−0.001 48
Expt. (Ref. 1)	254.4		
Expt. (Ref. 2)	257	−0.001 22	−0.001 36
Expt. (Ref. 3)	239	−0.001 37	−0.001 34
Expt. (Ref. 5)	255.0		
Expt. (Ref. 6)	255		

The symmetry-preserving elastic constants given in Table III can be used to generate three other parameters that are routinely accessible with hydrostatic EOS measurements, thereby providing an independent test for the quality of the present results. As was discussed in considerable detail by Jansen and Freeman,[34] the static-lattice bulk modulus B can be calculated from

$$B=\frac{C_3(C_{11}+C_{12})-2C_{13}^2}{(C_{11}+C_{12})+2C_{33}-4C_{13}}, \tag{6}$$

while the pressure derivatives of the hexagonal lattice constants are given by

$$a'\equiv\frac{\delta}{\delta P}\left(\frac{a}{a_0}\right)=\frac{C_{33}-C_{13}}{2C_{13}^2-C_{33}(C_{11}+C_{12})} \tag{7}$$

and

$$c'\equiv\frac{\delta}{\delta P}\left(\frac{c}{c_0}\right)=\frac{(C_{11}+C_{12})-2C_{13}}{2C_{13}^2-C_{33}(C_{11}+C_{12})}. \tag{8}$$

The values obtained here for these EOS related parameters are given in Table IV, along with previous theoretical estimates[15,21,22] and experimental data.[1–3,5,6] To avoid redundancy, Table IV does not include values derived from elastic constants other than the present results. On the basis of a carefull analysis of 16 experimental and theoretical values of B, including EOS and elastic constant measurements, Richet *et al.*,[6] concluded that the ''best'' estimate for B is 253 ± 1 GPa. The result derived from the cubic fit, $B=248.7$ GPa, only differs from that estimate by 1.7%. The predicted pressure derivatives of the lattice constants agree with the experiments to the extent that the experiments agree with each other.

B. High-pressure properties

Although the two-dimensional cubic function given in Eq. (1) provides a very good fit to the binding energy of corundum near the energy minimum, it cannot be expected to fit

TABLE V. Binding energy (E_b; Ry/molecule), c/a ratio, electronic energy band gap (E_g; eV), tetragonal shear modulus (C^t; GPa), and fitted pressure for each volume (V; bohr^3).

V	E_b	c/a	E_g	C^t	P
305.4613	−2.670 540	2.7303	5.38	186.7	−13.28
296.2981	−2.677 131	2.7260	5.74	187.4	−7.26
287.3200	−2.679 523	2.7211	6.13	189.5	−0.28
278.5251	−2.677 311	2.7159	6.51	197.7	7.79
269.9115	−2.670 021	2.7104	6.90	204.4	17.05
261.4774	−2.657 210	2.7048	7.30	218.9	27.67
245.1399	−2.612 792	2.6934	8.12	267.0	53.59
229.4976	−2.539 219	2.6853	8.97	329.4	87.02
207.3043	−2.359 807	2.6720	10.20	439.5	155.34
186.5900	−2.077 357	2.6584	10.53	469.2	252.74

the energies far from the minimum. For this reason, an alternative approach was used to extract the high-pressure EOS of corundum from the calculated binding energies. First, the four binding energies at each volume were fitted with a cubic function of a to calculate the minimum energy and c/a ratio at that volume. The electronic band gap for each volume was estimated by a simple linear interpolation. The cubic fit parameters were also used to obtain the tetragonal shear modulus at each volume from the equation

$$C^t = \frac{a_0^2}{12V_0}\left[\frac{\delta^2 E}{\delta a^2}\right]_V . \tag{9}$$

The binding energies, c/a ratios, band gaps, and tetragonal shear modulii obtained in this fashion are listed in Table V as functions of volume. The hydrostatic EOS was then determined by fitting the energies in Table V with a modified version[29] of the so-called universal EOS.[35] The standard deviation for that fit, shown in Fig. 2, was 0.1 mRy/molecule versus a total energy range of 6022 mRy/molecule. Pressures obtained from the EOS fit are listed in Table V for each of the volumes used in the calculations.

The four independent parameters of the modified universal EOS can be chosen to be the zero-pressure values for the

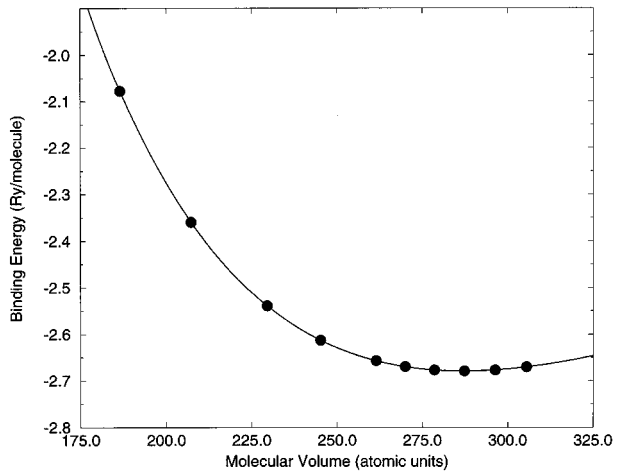

FIG. 2. Calculated binding energies (Ry/molecule) and fitted binding curve as a function of volume for corundum.

TABLE VI. Zero-pressure values for the volume (V_0; bohr^3/molecule), binding energy (E_0; Ry/molecule), bulk modulus (B_0; GPa), and pressure derivative of the bulk modulus (B_0') obtained from the modified universal EOS compared with previous electronic structure results and experiment.

Source	V_0	E_0	B_0	B_0'
LCGTO-FF (Present)	286.99	−2.679 436	243.8	4.305
OLCAO (Ref. 21)	287.3		242	3.24
LAPW+LO (Ref. 22)	282.0		257	4.05
Expt. (Ref. 1)	287.81		254.4	4.275

volume V_0, binding energy E_0, bulk modulus B_0, and pressure derivative of the bulk modulus B_0'.[36] These EOS fit parameters are listed in Table VI, along with results from other LDA electronic structure calculations[21,22] and experimental values from d'Amour *et al.*[1] The EOS fit values for V_0 and E_0 are in almost perfect agreement with the values obtained from the cubic fit. The only significant discrepancy between the two fits is in the bulk modulus; 243.8 GPa from the EOS fit versus 248.7 GPa from the more reliable cubic fit. The current fitted value of B_0' (4.305) is in good agreement with the measured value (4.275);[1] a particularly reassuring result given the important role played by this parameter in determining the EOS at very high pressures.

The fitted pressure versus volume curve is compared with 300 K data[1–6] in Fig. 3. For pressures up to about 20 GPa the data are fairly tightly grouped with small, systematic differences between the data sets that are most likely due to variations in either the samples or the equipment used. In this low pressure region, the fitted EOS passes roughly through the center of the data. For intermediate pressures, 20–60 GPa, all of the data are from two sets of quasihydrostatic experiments,[5,6] which should provide an upper bound to the 300 K hydrostat. In this intermediate pressure region, the theoretical EOS consistently lies along the lower edge of the rather widely scattered data, as expected. The very highest pressure points in Fig. 3 (60–200 GPa) are from a series of experiments that were conducted under nonhydrostatic conditions in an attempt to induce a crystallographic phase transition in ruby.[4] Thus, like the quasihydrostatic data, the highest pressure data should provide an upper bound to the 300 K hydrostat, which in turn should be an upper bound to the 0 K isotherm. Overall, the EOS obtained here from the parameters in Table VI agrees with the experimental data to the extent that can be expected given the known limitations of that data.

The c/a ratio and tetragonal shear modulus are plotted as functions of pressure in Fig. 4. The $P=0$ values for c/a (2.72) and C^t (190 GPa) are both in good agreement with the results found with the more precise two-dimensional cubic fit. The c/a ratio in Fig. 3 is a steadily decreasing function of pressure that varys by less than 3% over the entire 250 GPa range of the calculations. This nearly isotropic compression is consistent with existing experimental data[1–3] and with the small difference between the pressure derivatives of the hexagonal lattice constants found here with the cubic fit; see Table IV. The tetragonal shear modulus initially rises rapidly with pressure and then appears to level off by $P=250$ GPa. It would be very interesting to learn whether or not C_t eventu-

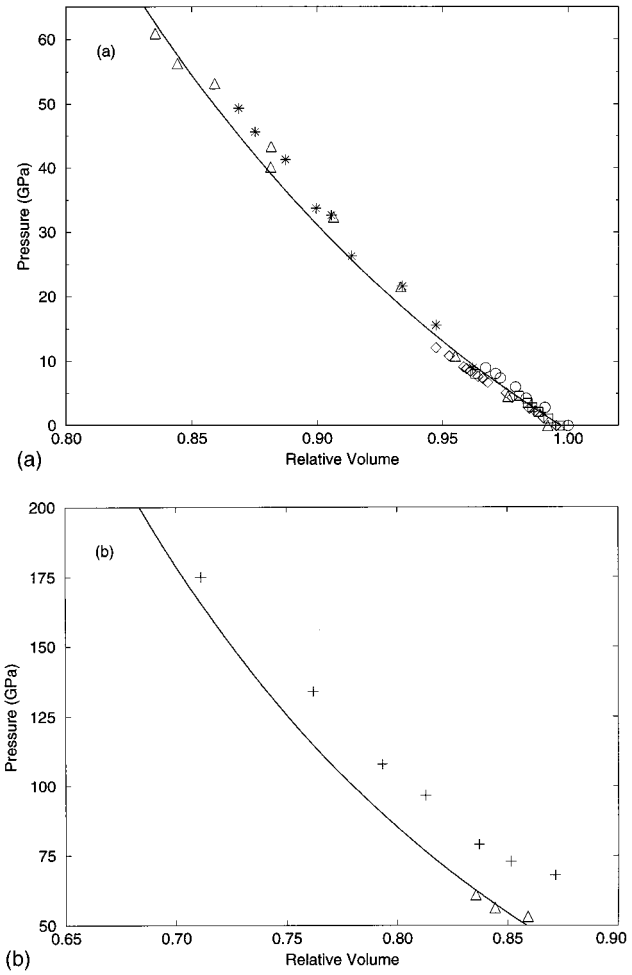

FIG. 3. Calculated pressure versus relative volume curve compared with 300 K data from Ref. 1 (circle), Ref. 2 (square), Ref. 3 (diamond), Ref. 4 (plus), Ref. 5 (triangle), and Ref. 6 (star); (a) low pressure region; (b) high pressure region. The reference volume is the room temperature volume from Ref. 1.

ally begins to decrease with pressure, in which case the unit cell might begin to distort rapidly.

The calculated fundamental band gap for corundum is plotted as a function of pressure in Fig. 5. (The complete band structure is not shown here because of the minimal number of k points sampled in the BZ.) At zero-pressure the present calculations yield a 6.14 eV direct band gap at the center of the BZ versus an experimental room temperature gap of 8.8 eV,[37] also at the zone center. This 30% underestimate of the band gap is typical for LDA calculations and is consistent with an earlier OLCAO calculation.[21] For pressures up to 150 GPa, the band gap remains direct and increases steadily to about 10.2 eV. By $P=250$ GPa, the band gap becomes indirect to a conduction state at the edge of the BZ; thereby accounting for the deviation in the curve between the two smaller volumes. This shift from a direct band gap to an indirect gap may signal the onset of a reordering of the energy bands in corundum,[38] which could also account for the softening of the tetragonal shear modulus in the same pressure range. Inspection of all forty calculated band gaps revealed that, for all of the volumes considered, the band gap decreases under uniaxial compression along the c axis with the volume held fixed. Although the band gap itself is underestimated in LDA calculations, the pressure derivative of the band gap is often quite realistic.[39] From the band gaps and pressures listed in Table V, the linear pressure coefficient of the band gap is estimated to be 5.1 meV/kbar at $P=0$.

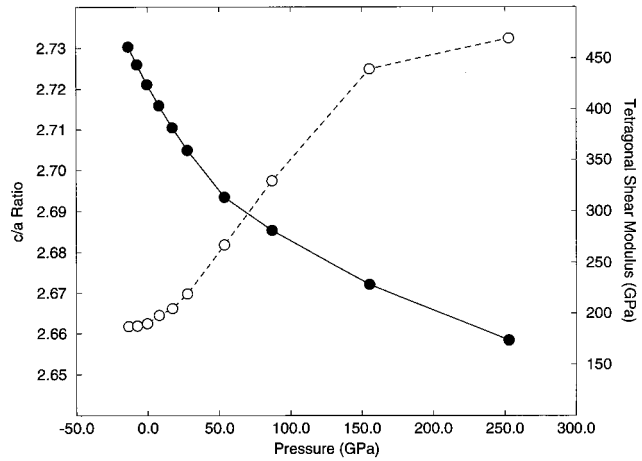

FIG. 4. Calculated c/a ratio (solid circles) and tetragonal shear modulus (open circles) versus pressure for corundum.

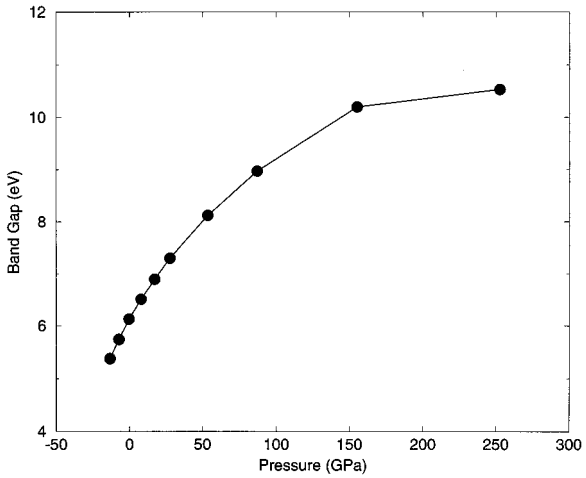

FIG. 5. Calculated electronic energy band gap versus pressure for corundum.

V. CONCLUSIONS

The LCGTO-FF calculations presented here for corundum have produced a number of predictions that are in extraordinary agreement with the existing experimental data; including 0.3% agreement for all of the lattice parameters and 5% agreement for the zero-pressure elastic properties. This level of agreement between theory and experiment establishes corundum as one of the few materials that do not exhibit any LDA-induced lattice contraction for nonrelativistic calculations.[29] In addition, this level of agreement with existing data lends plausibility to the predictions made here for properties that have not yet been measured. Thus, much effort has gone into extracting physical properties from the calculated values of E_b and E_g. These include zero-pressure values for the bulk modulus, the pressure derivative of the bulk modulus, the pressure derivatives of the hexagonal lattice parameters, and the linear pressure coefficient for the

fundamental energy band gap. An analytical EOS has also been generated from the calculated energies and has been used to determine the pressure dependences of the c/a ratio, band gap, and tetragonal shear modulus. In the 150→250 GPa pressure range, the band gap goes from direct to indirect and the tetragonal shear modulus shows signs of softening. Both of these effects could be due to the onset of a pressure induced reordering of the energy bands in that pressure range.

In spite of the great success achieved here in determining the properties of corundum, the calculated results contains a wealth of information that has not yet been extracted due to limitations of the analytical functions used to fit the data. For example, in the low-pressure region, the two dimensional cubic fit [Eq. (1) and Table I] should be substantially more accurate than the universal EOS fit (Table VI) and allows a description of nonisotropic distortions of the lattice. The cubic fit however is only valid near the energy minimum and thus can not be used to determine the high-pressure properties. One way of avoiding these limitations would be to use the calculated data[31] to develop model potentials for Al and O, which could then be used to predict additional properties for corundum. Such an effort, however, lies well outside the scope of the current investigation.

ACKNOWLEDGMENTS

Helpful conversations with S. B. Trickey are acknowledged. This work was supported by the U.S. Department of Energy.

[1] H. d'Amour, D. Schiferl, W. Denner, H. Schulz, and W. B. Holzapfel, J. Appl. Phys. **49**, 4411 (1978).
[2] L. W. Finger and R. M. Hazen, J. Appl. Phys. **49**, 5823 (1978).
[3] Y. Sato and S. Akimoto, J. Appl. Phys. **50**, 5285 (1979).
[4] A. P. Jephcoat, R. J. Hemley, and H. K. Mao, Physica B **150**, 115 (1988).
[5] J. Xu, High Temp. High Press. **19**, 661 (1987).
[6] P. Richet, J. Xu, and H. K. Mao, Phys. Chem. Minerals **16**, 207 (1988).
[7] For a review of early elastic constant data see O. L. Anderson, E. Schreiber, and R. C. Liebermann, Rev. Geophys. **6**, 491 (1968).
[8] J. H. Gieske and G. R. Barsch, Phys. Status Solidi **29**, 121 (1968).
[9] T. Goto, O. L. Anderson, I. Ohno, and S. Yamamoto, J. Geophys. Res. **94**, 7588 (1989).
[10] K. Iishi, Phys. Chem. Minerals **3**, 1 (1978).
[11] C. R. A. Catlow, R. James, W. C. Mackrodt, and R. F. Stewart, Phys. Rev. B **25**, 1006 (1982).
[12] H. A. Lauwers, L. Van Haverbeke, and M. A. Herman, J. Phys. Chem. Solids **44**, 489 (1983).
[13] A. Au and R. M. Hazen, Geophys. Res. Lett. **12**, 725 (1985).
[14] R. E. Cohen, Phys. Geophys. Res. Lett. **14**, 37 (1987).
[15] H. Cynn, D. G. Isaak, R. E. Cohen, M. F. Nicol, and O. L. Anderson, Am. Minerol. **75**, 439 (1990).
[16] T. Pilati, F. Demartin, and C. M. Gramaccioli, Acta. Crystallogr. A **49**, 473 (1993).
[17] H. Schober, D. Strauch, and B. Dorner, Z. Phys. B **92**, 273 (1993).
[18] R. W. G. Wyckoff, *Crystal Structures*, 2nd ed. (Interscience, New York, 1964), Vol. 2, p. 6.
[19] See, for example, S. Ciraci and I. P. Batra, Phys. Rev. B **28**, 982 (1983); and references therein.
[20] L. Salasco, R. Dovesi, R. Orlando, M. Causa, and V. R. Saunders, Mol. Phys. **72**, 267 (1991); see also, M. Causa, R. Dovesi, C. Roetti, E. Kotomin, and V. R. Saunders, Chem. Phys. Lett. **140**, 120 (1987).
[21] W. Y. Ching and Y. N. Xu, J. Am. Ceram. Soc. **77**, 404 (1994).
[22] F. C. Marton and R. E. Cohen, Am. Minerol. **79**, 789 (1994).
[23] J. C. Boettger, Int. J. Quantum Chem. Symp. **29**, 197 (1995).
[24] J. C. Boettger, Int. J. Quantum Chem. Symp. **27**, 147 (1993); also see J. C. Boettger and S. B. Trickey, Phys. Rev. B **32**, 1356 (1985); and J. W. Mintmire, J. R. Sabin, and S. B. Trickey, *ibid.* **26**, 1743 (1982).
[25] U. Birkenheuer, J. C. Boettger, and N. Rösch, J. Chem. Phys. **100**, 6826 (1994); and U. Birkenheuer, dissertation, TU München, 1994.
[26] L. Hedin and B. I. Lundqvist, J. Phys. C **4**, 2064 (1971).
[27] S. Huzinaga (unpublished).
[28] The contraction pattern of the *s* part of the orbital basis set used here for Al was taken from T. H. Dunning and P. J. Hay, in *Methods of Electronic Structure Theory*, edited by H. F. Schaefer III (Plenum, New York, 1977); p. 1.
[29] J. C. Boettger and S. B. Trickey, Phys. Rev. B **53**, 3007 (1996); see also, J. C. Boettger and S. B. Trickey, *ibid.* **51**, 15 623 (1995).
[30] J. C. Boettger, Phys. Rev. B **53**, 13 133 (1996); see also, J. C. Boettger, U. Birkenheuer, N. Rösch, and S. B. Trickey, Int. J. Quantum Chem. Symp. **28**, 675 (1994).
[31] The forty calculated values of E_b and E_g can be obtained in a tabular form from the author.
[32] *Thermophysical Properties of Matter*, edited by Y. S. Touloukian, R. K. Kirby, R. E. Taylor, and T. Y. R. Lee (Plenum, New York, 1977), Vol. 13, p. 176.
[33] G. K. White and R. B. Roberts, High Temp. High Press. **15**, 321 (1983).
[34] H. J. F. Jansen and A. J. Freeman, Phys. Rev. B **35**, 8207 (1987).
[35] P. Vinet, J. Ferrante, J. H. Rose, and J. R. Smith, J. Phys. Condens. Matter **1**, 1941 (1989).
[36] J. C. Boettger and D. C. Wallace, Phys. Rev. B (to be published).
[37] R. H. French, J. Am. Ceram. Soc. **73**, 477 (1990).
[38] W. G. Zittel, J. Meyer-ter-Vehn, J. C. Boettger, and S. B. Trickey, J. Phys. F **15**, L247 (1985).
[39] S. B. Trickey, A. K. Ray, and J. P. Worth, Phys. Status Solidi B **106**, 613 (1981); K. J. Chang, S. Froyen, and M. L. Cohen, Solid State Commun. **50**, 105 (1984); S. Lee, J. Sanchez-Dehasa, and J. D. Dow, Phys. Rev. B **32**, 1152 (1985).